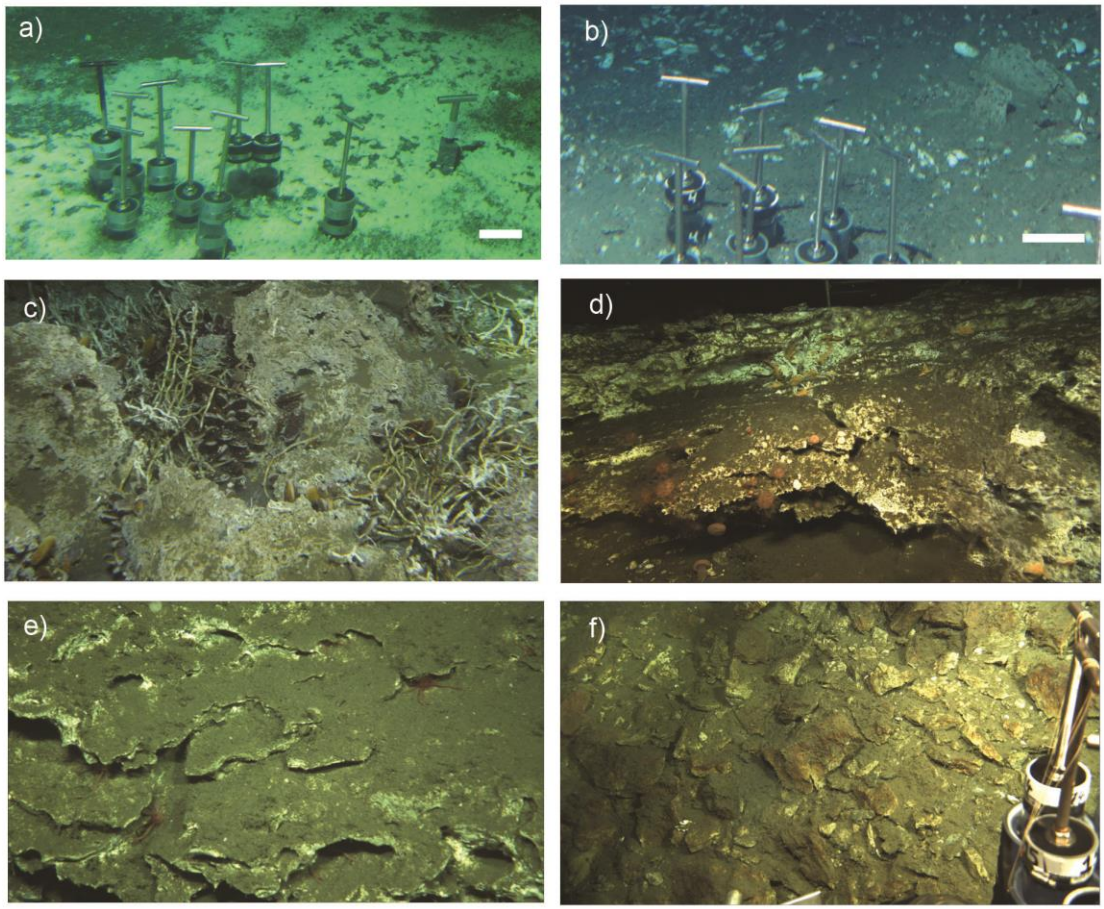

Supplementary Figure 1. Sampling sites representative of those discussed in this study. **(a)** A white bacterial mat indicative of an active methane seep at 802 m water depth at Hydrate Ridge South; sample A.Sed-3452 was collected from this site. **(b)** A vesicomyid clam bed at an active methane seep at Hydrate Ridge South seen during AD 4629 (800 m water depth). **(c)** Active carbonates at Mound 12, Costa Rica, at a water depth of 997 m. **(d)** Exhumed active carbonate at Hydrate Ridge South (804 m water depth). Low-activity carbonates at Hydrate Ridge are seen in both **(e)** cohesive sediment-draped pavements at 829 m water depth, and **(f)** deposits of fragmented carbonates at 842 m water depth. **(a)** and **(b)** scale bars are 10 cm; **(c)** and **(d)** foreground scenes are approximately 2.5 m and 4 m across, respectively; **(e)** and **(f)** are approximately 1 m across.

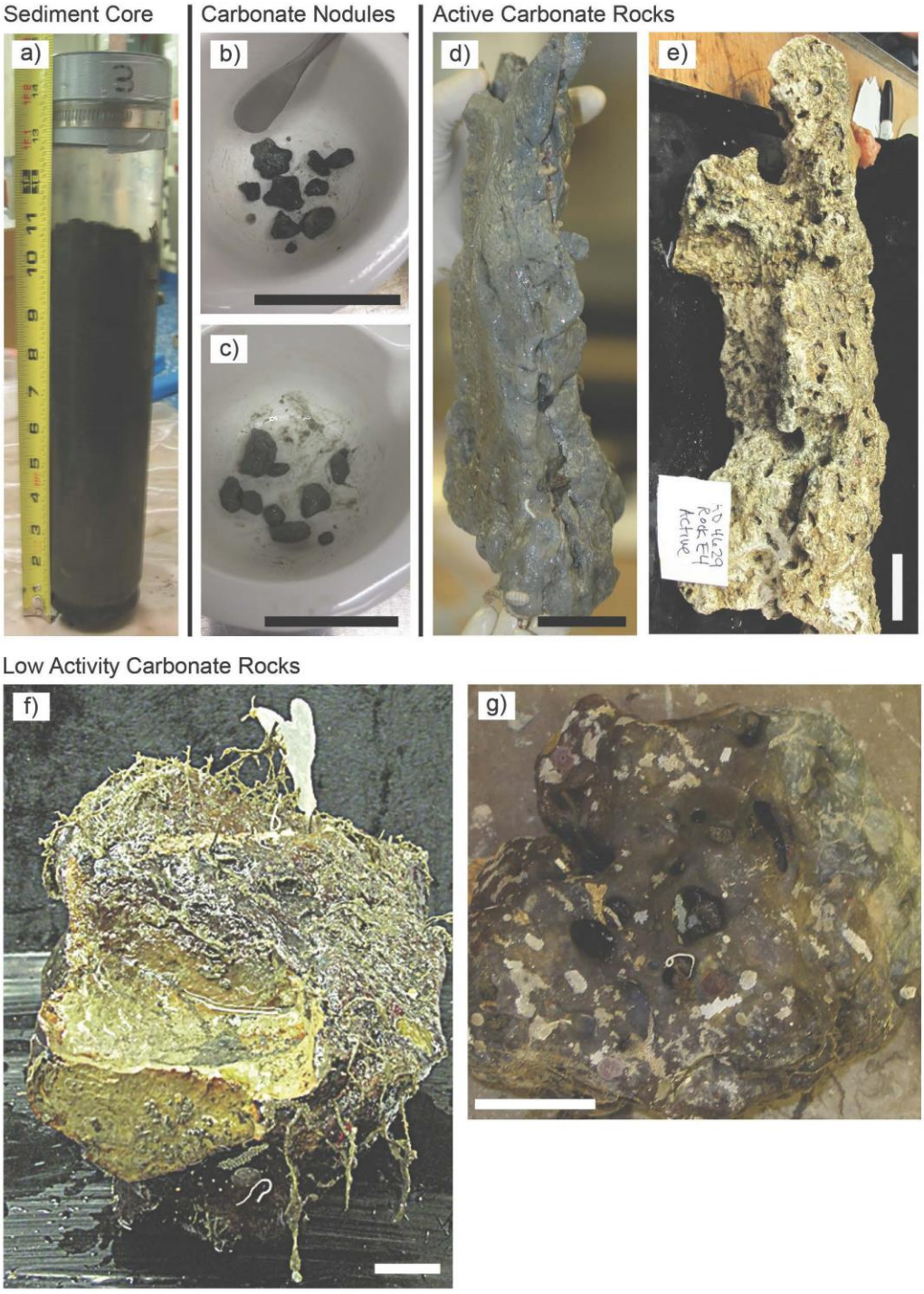

Supplementary Figure 2. Representative samples analyzed in this study. **(a)** Active 30-cm sediment core PC3 from AD 4511, 997 m water depth, Costa Rica Mound 12. **(b)** Nodules from AD 4511 PC3, Costa Rica, acquired from the core's 12-15 cm horizon. **(c)** Nodules from AD 4587 PC18 3-6 cm horizon, 996 m water depth, Mound 12, Costa Rica. **(d)** Active massive carbonate rock A.Carb-2840 collected from Mound 12, 997 m water depth, Costa Rica during AD 4501. **(e)** Active porous carbonate rock A.Carb-3439 from AD 4629, 800 m water depth, Hydrate Ridge. **(f)** Low activity massive carbonate rock L.Carb-3604 from AD 4633, 623 m water depth, Hydrate Ridge. **(g)** Low activity massive carbonate rock L.Carb-2787 from Eel River Basin, water depth 540 m. Scale bars are 5 cm.

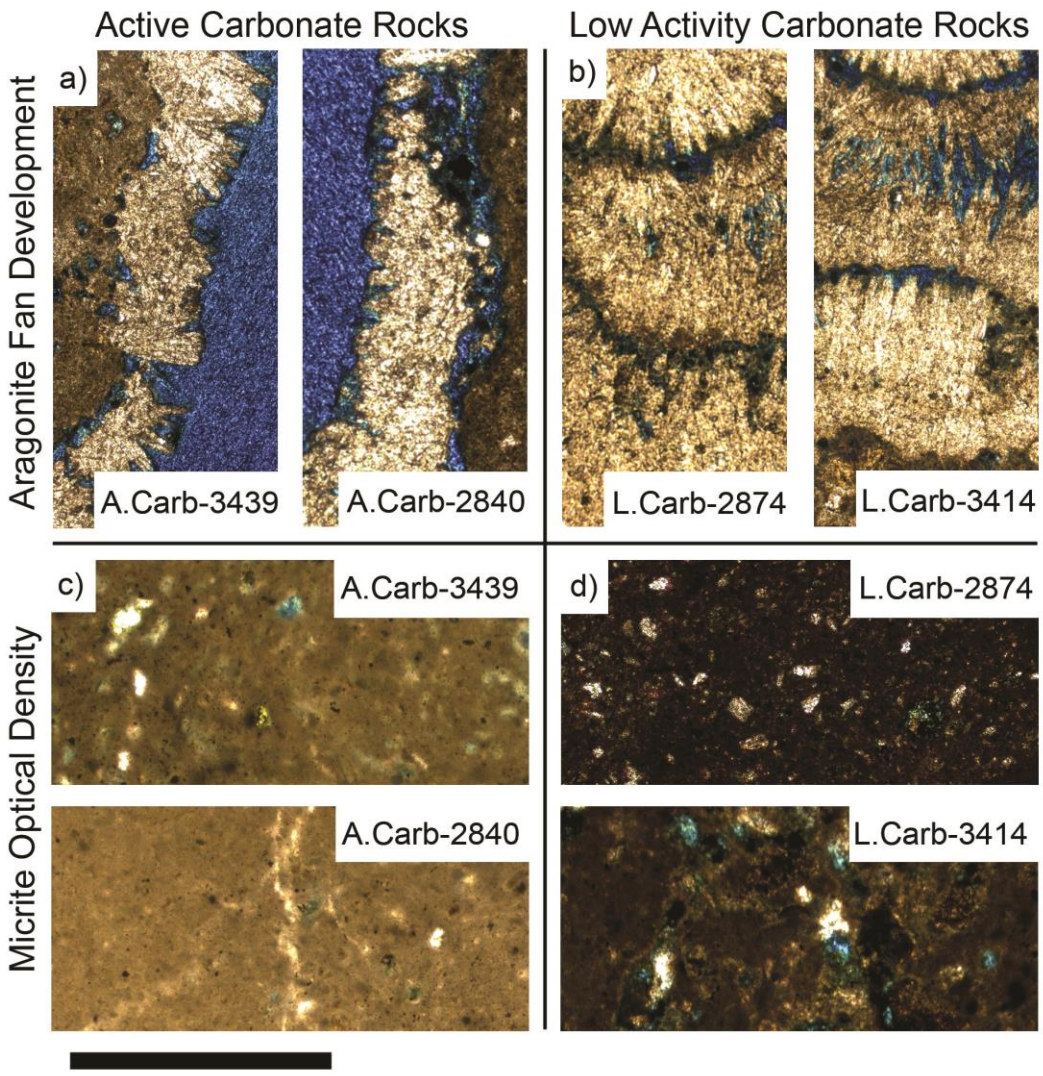

Supplementary Figure 3. Differences among active carbonate (**a** and **c**) and low-activity carbonate (**b** and **d**) thin sections. Images in the top panels (**a** and **b**) show the differences in aragonite fan development; those in the bottom panels (**c** and **d**) demonstrate the variation in micrite optical density. All images were taken at the same exposure and exhibit no post-processing; blue color represents the embedding matrix, which can be interpreted as pore space. Scale bar = 0.5 mm.

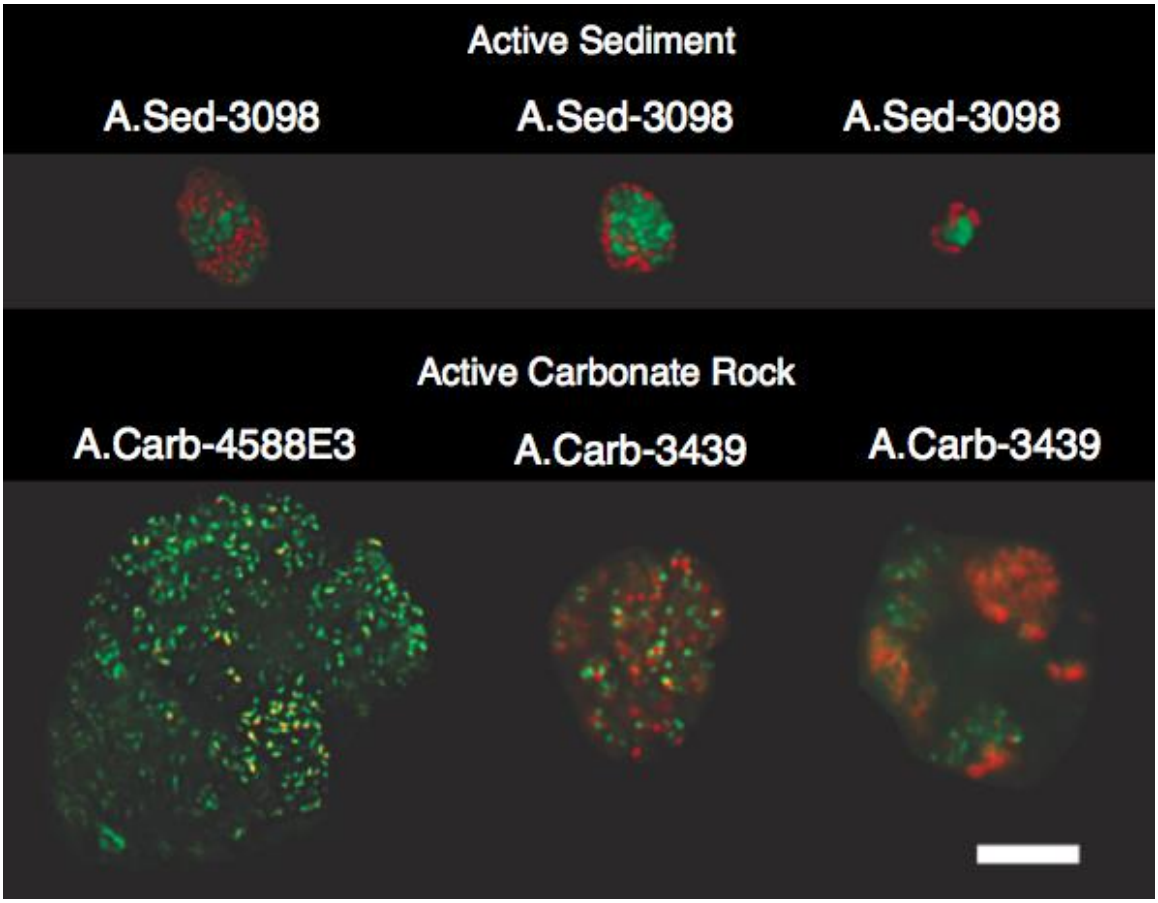

Supplementary Figure 4. Morphological comparisons between sediment- and carbonate-hosted microbial aggregates. CARD-FISH images of Archaea (Arch915 probe, green) and *Desulfosarcina / Desulfococcus* (DSS658 probe, red) aggregates from active sediment (A.Sed-3098) and active carbonate (A.Carb-4588E3, A.Carb-3439) samples. Scale bar = 5 μm.

Supplementary Table 1. Details of the 24 samples used in this study, including active sediment, active nodules, active porous carbonate, active massive carbonate, low activity sediment, and low activity massive carbonate. Serial numbers are unique identifier numerals preceded by an acronym of the sample's seep activity designation and degree of lithification. A.Sed = active sediment, A.Nod = active nodule, A.Carb = active carbonate, L.Sed = low activity sediment, and L.Carb = low activity carbonate. Definitions of seep activity and lithification designators are provided in the main and supplemental text. X = X-ray diffraction, CC = cell counts and aggregate characterization, PM = attempted *pmoA* gene amplification, PP = porosity and permeability tests, TS = petrographic thin section analysis, 16S = 16S rRNA gene clone library sequencing, 454 = pyrotag sequencing, SA = aggregate spatial arrangement study, ^{14}C = $^{14}CH_4$ radiolabel rate measurement, NS = CARD-FISH / nanoSIMS analysis, BV = aggregate biovolume calculation.

Serial #	Sample ID	Seep Activity	Lithification	Sampling Location	Analyses Performed
A.Sed-3098	AD 4511 PC3 9-12 cm	Active	Sediment	Costa Rica	X, CC, BV
A.Sed-3452	AD 4629 PC8 3-6 cm	Active	Sediment	Hydrate Ridge	X, CC, PM
A.Sed-3730	AD 4635 PC16 0-6 cm	Active	Sediment	Hydrate Ridge	16S
A.Sed-5128	J2 593 E3 PC 40 0-12 cm	Active	Sediment	Hydrate Ridge	CC, ^{14}C
A.Nod-2518	AD 4249 PC8 3-6 cm	Active	Nodule	Hydrate Ridge	CC, 16S
A.Nod-2688	AD 4256 PC29 6-9 cm	Active	Nodule	Eel River Basin	CC
A.Nod-3099	AD 4511 PC3 12-15 cm	Active	Nodule	Costa Rica	X, CC, BV, PM
A.Nod-3294	AD 4587 PC18 3-6 cm	Active	Nodule	Costa Rica	X, NS
A.Carb-3439	AD 4629 Jefe	Active	Porous Carbonate	Hydrate Ridge	TS, CC, BV, 16S, NS, 454
A.Carb-5305	J2 593 E7A B8B	Active	Porous Carbonate	Hydrate Ridge	X, CC, ^{14}C
A.Carb-2840	AD 4501 L1	Active	Massive Carbonate	Costa Rica	TS, PM
A.Carb-2871	AD 4502 L2	Active	Massive Carbonate	Costa Rica	CC
A.Carb-3460	AD 4589 R8	Active	Massive Carbonate	Costa Rica	TS
A.Carb-4588E3	AD 4588E3	Active	Massive Carbonate	Costa Rica	X, PP, CC
A.Carb-5152	J2 593 E4B B24	Active	Massive Carbonate	Hydrate Ridge	PP, CC, BV, ^{14}C
L.Sed-2939	AD 4504 PC3 3-6 cm	Low Activity	Sediment	Costa Rica	CC
L.Sed-5043	J2 593 E1 PC2 0-12 cm	Low Activity	Sediment	Hydrate Ridge	CC, ^{14}C, PM
L.Carb-2719	AD 4256 G4	Low Activity	Massive Carbonate	Eel River Basin	PP
L.Carb-2787	AD 4258 G2	Low Activity	Massive Carbonate	Eel River Basin	PP
L.Carb-2874	AD 4502 S3	Low Activity	Massive Carbonate	Costa Rica	X, TS, CC
L.Carb-3414	AD 4629 E3B	Low Activity	Massive Carbonate	Hydrate Ridge	TS, PM
L.Carb-3604	AD 4633 L1	Low Activity	Massive Carbonate	Hydrate Ridge	X, CC, 16S
L.Carb-5028	J2 593 E1A B12	Low Activity	Massive Carbonate	Hydrate Ridge	PP, CC, ^{14}C
L.Carb-5473	J2 593 E10B B15	Low Activity	Massive Carbonate	Hydrate Ridge	PP

Supplementary Table 2. Porosity and permeability results from core plug analysis of several carbonate samples. Vuggy active porous carbonates were not testable with this method due to structural instability caused by macroscale voids.

Sample	Sampling Location	Description	Porosity (%)	Permeability (m^2)
L.Carb-2787	Eel River Basin	Low Activity Massive	4.9	$3x10^{-18}$
L.Carb-5028	Hydrate Ridge	Low Activity Massive	8.9	$4x10^{-18}$
L.Carb-2719	Eel River Basin	Low Activity Massive	8	$1.1x10^{-17}$
L.Carb-5473	Hydrate Ridge	Low Activity Massive	16.6	$3.5x10^{-17}$
A.Carb-5152	Hydrate Ridge	Active Massive	34.4	$1.7x10^{-15}$
A.Carb-4588E3	Costa Rica	Active Massive	25	$4.9x10^{-15}$

Supplementary Table 3. Cell counts from ten samples examined in this study. Values represent cumulative counts over 25 fields of view. Absolute cell count numbers are not directly comparable between samples, as different volumes of material were concentrated on filters for each sample; rather, the proportion of single cells can be compared among different samples.

Sample	Aggregate-based Cells	Single Cells	Proportion of Single Cells
A.Sed-3098	2044	17	0.80%
A.Sed-5128	897	9	1%
A.Nod-2518	629	5	0.79%
A.Nod-3099	3138	26	0.83%
A.Carb-3439	1887	13	0.69%
A.Carb-5152	342	7	2%
L.Sed-2939	487	65	13.35%
L.Sed-5043	620	61	9.84%
L.Carb-2874	342	52	15.20%
L.Carb-3604	1002	143	14.27%

Supplementary Table 4. ^{13}C and ^{15}N atom percent enrichment values for aggregates from labeled (2 mM $^{15}NH_4Cl$, 0.74 mM $^{13}CH_4$, and 0.74 mM $^{12}CH_4$) and unlabeled (2 mM $^{14}NH_4Cl$ and 1.48 mM $^{12}CH_4$) incubations of sample A.Carb-3439 at 4 °C for 27 months under anoxic conditions. Values represent full aggregate analyses, incorporating data from all nanoSIMS cycles within a defined region of interest that was informed by CARD-FISH biomass identifications. Aggregate 17 refers to the aggregate in panel c of Fig. 2, aggregate 25 to panel a, and aggregates 31a and b to cell aggregates seen on the left and right of panel b, respectively. *Clostridia* spores (n=5 in both cases) were added following experimental treatment and demonstrate consistent measurement conditions.

^{15}N, ^{13}C Labeled Incubation Aggregates		
	^{13}C atm %	^{15}N atm %
Aggregate 17	1.15	81.48
Aggregate 25	0.87	81.31
Aggregate 31a	0.80	69.42
Aggregate 31b	1.03	69.51
Clostridia spore avg	0.77	0.37
Unlabeled Incubation Aggregates		
	^{13}C atm %	^{15}N atm %
Aggregate 16	0.48	0.35
Aggregate 23	0.66	0.37
Aggregate 24	0.51	0.33
Clostridia spore avg.	0.76	0.37

Supplementary Methods

Phylogenetic Analysis
Polymerase chain reaction (PCR) was performed in order to amplify bacterial and archaeal 16S rRNA genes. Bacterial PCR used the 27F[1] (5'-AGAGTTTGATCCTGGCTCAG-3') / 1492R[2] (5'-GGYTACCTTGTTACGACTT-3') primers, while archaeal PCR used 8F[3] (5'-TCCGGTTGATCCTGCC-3') / 958R[2] (5'-YCCGGCGTTGAMTCCAATT-3') primers. New England BioLab's *Taq* DNA Polymerase (NEB, Ipswich, MA) was used in all PCRs. PCR was run on an Eppendorf Mastercycler Ep Gradient S thermocycler as follows: an initial denaturation of 2 minutes at 95 °C; 30 cycles of 15 seconds at 94 °C, 30 seconds at 54 °C, and 45 seconds at 72 °C; and a final 4 minute elongation at 72 °C.

Sequences were aligned with Mothur[4] and checked for chimeras with bellerophon, pintail, and slayer chimera check programs. Non-chimeric sequences were imported to ARB[5], aligned in accordance with the Silva 115 NR99 database.

454 Sequencing
PCR reactions (50 µl) for 454 sequencing were prepared with 20 ng of template DNA, 5 µl 10x buffer, 1 µl dNTP mix (10 mM each), 4 µl MgCl (25 mM), 1 µl forward primer (10 mM), 1 µl reverse primer (10 mM), 0.2 µl Taq polymerase and 1.5 µl BSA, and 1 µl (10 mM) of each of the universal primers targeting the V6-V8 region of the bacterial and archaeal 16S rRNA gene[6]: 926F (5'-AAACTYAAAKGAATTGRCGG-3') and 1392R (5'-ACGGGCGGTGTGTRC-3') modified on the 5' end to contain 454 sequencing adaptor sequences. The reverse primer also contained a 5–6 base sample-specific barcode sequence. The PCR program included one cycle at 95 °C for 3 minutes, followed by 30 cycles at 95 °C for 30 seconds, 55 °C for 30 seconds, and 75 °C for 30 seconds, and then a final extension at 74 °C for 10 minutes. After amplification, amplicons were pooled and sequenced using the Roche 454 GS-FLX Titanium platform (Roche Diagnostics, Castle Hill, NSW, Australia) at the Australian Centre for Ecogenomics.

Amplicons derived from 454 sequencing were processed using the Quantitative Insights Into Microbial Ecology (QIIME) package[7]. Chimera detection was performed using UCHIME[8] against a modified Silva115 NR99 reference database[9]. The Silva 115 NR99 database had been filtered to include only those sequences with pintail value >75, and appended with 1197 high-quality, full-length sequences from the Orphan lab, increasing the database coverage of common methane seep taxa. This modified database, including taxonomies, is available upon request.

CARD-FISH
Domain and group-specific probes were used to visualize Archaea (Arch915[10] – Alexa green: 5'-GTGCTCCCCCGCCAATTCCT-3'), ANME-2 (ANME2-538[11] – Alexa green 5'-GGCTACCACTCGGGCCGC-3'), and *Desulfosarcina* / *Desulfococcus* (DSS658[12] – Alexa red: 5'-TCCACTTCCCTCTCCCAT-3'). 1 µl of probe was added to 300 µl of hybridization buffer (50% formamide by volume), and 20 µl of the mixture was placed on

the sample surface. The amplification buffer mix was prepared by mixing 600 µl amplification buffer with 6 µl dilute H_2O_2 (200 µl PBS + 6 µl 30% H_2O_2), and 1 µl of the appropriate tyramide fluorochrome (Alexa green for Arch915 and ANME2-538, Alexa red for DSS658). Probe-free negative controls to test for endogenous peroxidases were also processed, and no fluorescence signal was observed using the same exposure settings. ANME-1 FISH analysis was conducted as in Pernthaler et al.[13] and utilized the ANME-1 350 probe[14] Cy3 5'-AGTTTTCGCGCCTGATGC-3' with 40% formamide hybridization buffer.

$^{14}CH_4$ Rate Measurements

Radiolabeled methane (1 ml of $^{14}CH_4$ dissolved in seawater, corresponding to an activity of 52 kBq) was injected into each incubation bottle and samples were placed at 4 °C. At the designated time point (3 and 7 days for anaerobic incubations, 1.875 and 4 days for aerobic incubations), 2.5 ml of 2.5% (w/w) NaOH was injected to stop microbial activity. The relatively extended incubation durations likely encompass multiple stages of growth, with rates likely decreasing as methane was consumed. Thus, the reported average growth rates represent a potential underestimate of maximum growth rates under conditions of constant 2.2 mM methane supply. Each sample's headspace was purged with airflow through an 850 °C quartz tube furnace filled with Cu(II) oxide, combusting unused $^{14}CH_4$ to $^{14}CO_2$, which was collected in two sequential 23-ml scintillation vials pre-filled with 7 ml phenylethylamine and 1 ml 2-methoxyethanol. 10 ml of scintillation cocktail (Ultima Gold XR, PerkinElmer) was added, and the activity attributable to $^{14}CO_2$ was measured by scintillation counting 24 hours later (Beckman Coulter LS 6500 Multi-Purpose Scintillation Counter, 10 minute analysis per sample).

To quantify the $^{14}CO_2$ and $H^{14}CO_3^-$ produced during the incubation period, each sample was uncapped and the entire volume was transferred into a 250-ml Erlenmeyer flask along with 1 drop of antifoam. 5 ml of 6M HCl was added and the flask was immediately closed with a rubber stopper, two clamps, and parafilm to prevent gas escape. The flask was placed on a shaking table (60 rpm) at room temperature for 24 hours. A 7-ml scintillation vial, pre-filled with 1 ml of 2.5% NaOH and 1 ml of phenylethylamine, was suspended from the rubber stopper inside the flask to collect $^{14}CO_2$ generated by the acidification. 5 ml of scintillation cocktail was added, and the vial was measured by scintillation counting 24 hours later. This method has been shown to recover an average of 98% of $^{14}CO_2$[15].

Finally, six of the sterilized control incubations (four anaerobic, two aerobic) were set aside after $^{14}CH_4$ addition for gas chromatography to determine the initial concentration of methane gas. 400 µl was injected into a gas chromatograph (Shimadzu GC-2014), equipped with a packed stainless steel Supelco Custom Column (50/50 mixture, 80/100 Porapak N support, 80/100 Porapak Q column, 6 ft x 1/8 in) and a flame ionization detector. The carrier gas was helium at a flow rate of 30 ml min^{-1}. The column temperature was 60 °C. Results were scaled based on comparison with standards of known methane concentrations (10 and 100 ppm; Matheson Tri-Gas, Twinsburg, OH).

Supplementary References

1. Lane, D. J. *et al.* Rapid determination of 16S ribosomal RNA sequences for phylogenetic analyses. *Proc. Natl Acad. Sci. USA* **82,** 6955–6959 (1985).
2. DeLong, E. F. Archaea in coastal marine environments. *Proc. Natl Acad. Sci. USA* **89,** 5685–5689 (1992).
3. Teske, A. *et al.* Microbial Diversity of Hydrothermal Sediments in the Guaymas Basin: Evidence for Anaerobic Methanotrophic Communities. *Appl. Environ. Microb.* **68,** 1994–2007 (2002).
4. Schloss, P. D. *et al.* Introducing mothur: open-source, platform-independent, community-supported software for describing and comparing microbial communities. *Appl. Environ. Microb.* **75,** 7537–7541 (2009).
5. Ludwig, W. *et al.* ARB: a software environment for sequence data. *Nucleic Acids Res.* **32,** 1363–1371 (2004).
6. Engelbrektson, A. *et al.* Experimental factors affecting PCR-based estimates of microbial species richness and evenness. *ISME* **4,** 642–647 (2010).
7. Caporaso, J. G. *et al.* QIIME allows analysis of high-throughput community sequencing data. *Nature Methods* **7,** 335–336 (2010).
8. Edgar, R. C., Haas, B. J., Clemente, J. C., Quince, C. & Knight, R. UCHIME improves sensitivity and speed of chimera detection. *Bioinformatics* **27,** 2194–2200 (2011).
9. Quast, C. *et al.* The SILVA ribosomal RNA gene database project: improved data processing and web-based tools. *Nucleic Acids Res.* **41,** D590–D596 (2013).
10. Stahl, D. A. & Amann, R. *Development and application of nucleic acid probes* In: Nucleic acid techniques in bacterial systematics. E. Stackebrandt & M. Goodfellow (eds). Chichester, UK: Wiley (1991).
11. Treude, T., Knittel, K., Blumenberg, M., Seifert, R. & Boetius, A. Subsurface Microbial Methanotrophic Mats in the Black Sea. *Appl. Environ. Microb.* **71,** 6375–6378 (2005).
12. Ravenschlag, K., Sahm, K., Knoblauch, C., Jørgensen, B. B. & Amann, R. Community Structure, Cellular rRNA Content, and Activity of Sulfate-Reducing Bacteria in Marine Arctic Sediments. *Appl. Environ. Microb.* **66,** 3592–3602 (2000).
13. Pernthaler, J., Glöckner, F.-O., Schönhuber, W. & Amann, R. Fluorescence *in situ* hybridization (FISH) with rRNA-targeted oligonucleotide probes. *Methods Mol. Biol.* **30,** 207–226 (2001).
14. Boetius, A. *et al.* A marine microbial consortium apparently mediating anaerobic oxidation of methane. *Nature* **407,** (2000).
15. Treude,T., Boetius, A., Knittel, K., Wallmann, K., & Jørgensen, B.B. Anaerobic oxidation of methane above gas hydrates at Hydrate Ridge, NE Pacific Ocean. *Mar. Ecol. Prog. Ser.* **264,** 1–14 (2003).